Geophysical Journal International

Geophys. J. Int. (2019) **219,** 1043–1055
Advance Access publication 2019 July 30
GJI Gravity, Geodesy and Tides

doi: 10.1093/gji/ggz346

A non-perturbative method for gravitational potential calculations within heterogeneous and aspherical planets

Matthew Maitra and David Al-Attar

Department of Earth Sciences, Bullard Laboratories, University of Cambridge, Madingley Road, Cambridge CB3 OEZ, United Kingdom.
E-mail: mam221@cam.ac.uk

Accepted 2019 July 26. Received 2019 July 22; in original form 2019 April 2

SUMMARY

We present a numerically exact method for calculating the internal and external gravitational potential of aspherical and heterogeneous planets. Our approach is based on the transformation of Poisson's equation into an equivalent equation posed on a spherical computational domain. This new problem is solved in an efficient iterative manner based on a hybrid pseudospectral/spectral element discretization. The main advantage of our method is that its computational cost reflects the planet's geometric and structural complexity, being in many situations only marginally more expensive than boundary perturbation theory. Several numerical examples are presented to illustrate the method's efficacy and potential range of applications.

Key words: Geopotential theory; Numerical solutions.

1 INTRODUCTION

The calculation of a planet's gravitational potential is required in diverse areas of geophysics and planetary science, including studies of free oscillation seismology (e.g. Woodhouse & Dahlen 1978), body tides (e.g. Wahr 1981), rotational dynamics (e.g. Smith 1977), orbital evolution (e.g. Kaula 1964) and glacial isostatic adjustment (e.g. Peltier 1974). Neither the Earth nor any other planetary body of interest is geometrically spherical, where we follow the terminology of Al-Attar & Crawford (2016) and define a planet to be geometrically spherical if its internal and external boundaries form a series of concentric spheres. Within a geometrically spherical planet Poisson's equation can be reduced in an exact manner to a decoupled system of ordinary differential equations for the spherical harmonic coefficients of the potential. These differential equations can be solved using numerical quadrature, making it easy to calculate the planet's gravitational potential to any desired level of accuracy.

A number of approaches have been developed to account for asphericity within calculations of the gravitational potential. It is most common to assume the deviation of a boundary from an appropriate reference sphere to be small and determine its contribution to the gravitational potential using first-order boundary perturbation theory. In fact, for many applications, lateral variations in density are also regarded as first-order quantities, and this allows for the asphericity of the planet to be handled with minimal effort. Higher-order extensions of this boundary perturbation theory have been developed (e.g. Nakiboglu 1982; Chambat & Valette 2005) and the improvements over the first-order theory are significant for some terrestrial applications (e.g. Mitrovica *et al.* 2005; Chambat *et al.* 2010). The use of higher-order boundary perturbation theory, however, is both time-consuming and cumbersome, particularly when the coupling of such calculations into dynamic problems is considered.

Non-perturbative methods for calculating the external gravitational potential of aspherical bodies have been described a number of times in both the geophysics and planetary science literature. This includes, for example, the work of Parker (1973), Parker & Shure (1985), Martinec *et al.* (1989) and Balmino (1994) based on spectral expansions of the exterior gravitational potential of piecewise homogeneous bodies, and studies by Barnett (1976), Waldvogel (1979) and Werner (1994) using homogeneous polyhedral models for which the necessary integrals can be performed analytically. Whilst these methods are useful within their intended applications it seems unlikely that they can be readily extended to the calculation of the internal gravitational potential of a general heterogeneous planet. We note, however, that the method of Hubbard (2012, 2013), which is based on a combination of spectral and multipole expansions, can be applied to ellipsoidally symmetric bodies, and allows for accurate calculation of both the internal and external potential.

It is only quite recently that non-perturbative methods for calculating the internal gravitational potential of aspherical planets have been considered, this being motivated largely by the desire to model their dynamics without unnecessary approximations. At first sight, it might seem that this should be a simple problem. Indeed, we need only consider a linear partial differential equation with constant coefficients, whereas problems that are ostensibly far more complicated are now solved routinely using numerical methods. The difficulty with our problem, however, is that Poisson's equation is not defined in a finite domain, but within all of space. Of course, one could attempt to approximate the

whole of space by a sufficiently large computational domain, but this has been shown to be both inaccurate and inefficient (Gharti & Tromp 2017).

Within the geophysics literature three main approaches to this 'infinite-domain problem' have been discussed. First, Chaljub & Valette (2004) used a Dirichlet-to-Neumann (DtN) map to reduce Poisson's equation in $\mathbb{R}^3$ to an equivalent problem defined within a finite spherical domain containing the body of interest. The DtN map introduces non-local boundary terms into the problem, which comes with an associated computational cost. Chaljub & Valette's approach seems to have been impractical for its original application to long period seismology, but it has subsequently been employed in quasi-static deformation calculations by Métivier *et al.* (2006), Al-Attar & Tromp (2014), Crawford *et al.* (2016) and Crawford *et al.* (2018).

A second approach to calculating the internal potential field was described by Latychev *et al.* (2005) within their finite-volume method for modelling glacial isostatic adjustment. Here the internal gravitational potential was obtained through direct numerical evaluation of the Newtonian potential integrals at each point within the body. This method, however, is rather costly and care is needed in accounting for the singular nature of the integrands.

Most recently, a powerful approach known as the 'spectral infinite-element method' has been described within a series of papers by Gharti & Tromp (2017), Gharti *et al.* (2018) and Gharti *et al.* (2019). This is a variant of the infinite-element method developed within the engineering literature (e.g. Bettess 1977; Beer & Meek 1981; Medina & Taylor 1983) and reduces the exterior problem to the addition of a single layer of elements onto the interior domain, but without the need for non-local boundary terms. Numerical tests show this method to be both accurate and comparatively efficient while offering the flexibility to calculate the gravitational potential of an almost arbitrarily complex object.

Given the preceding comments it might seem that there is no problem left to solve. But this view leaves us with a rather stark gap in computational cost: within a geometrically spherical planet the gravitational potential can be determined in an almost trivial manner using spherical harmonic expansions, while in an aspherical planet the problem requires the assembly and solution of a large system of linear equations associated with the spectral-infinite-element discretization. The aim of this paper is to present an alternative method for gravitational potential calculations that fills out the middle ground, providing a numerically exact solution to the problem, but with a computational cost that reflects the planet's geometric complexity. In doing this we must sacrifice some generality in the planet's form, but will see that a usefully large class of structures can still be accounted for. The solution is 'numerically exact' in the sense that the only source of error is truncation of the radial and angular bases on which the problem is discretized: by taking sufficiently many terms in the expansion we can, in principle, achieve any desired level of accuracy.

The key idea in our method is the transformation of Poisson's equation into a new equation defined in a geometrically spherical reference domain (*cf.* Woodhouse 1976; Jobert 1976; Takeuchi 2005; Al-Attar & Crawford 2016; Leng *et al.* 2019). The introduction of such a mapping is similar to, and can be seen as a generalization of, Clairaut's approach to ellipsoidal equilibrium figures (e.g. Clairaut 1743; Chambat & Valette 2005). Whilst this transformed equation has laterally varying and tensorial coefficients, the geometrical sphericity of its domain means that it can be solved numerically using an approach based on generalized spherical harmonic (GSPH) expansions combined with a spectral element discretization in the radial co-ordinate (e.g. Al-Attar & Tromp 2014; Crawford *et al.* 2018). The lateral heterogeneity of the equation's coefficients leads to coupling between the different spherical harmonic orders and degrees, but the resulting linear system can be solved using a pre-conditioned iterative method similar to that of Al-Attar *et al.* (2012). Crucially, the closer the planet is to being geometrically spherical, the more quickly the iteration converges.

2 THEORY

2.1 Poisson's Equation for the gravitational potential

We begin by recalling the Poisson equation governing a planet's gravitational potential. The planet is assumed to occupy a compact subset $\mathcal{M} \subseteq \mathbb{R}^3$ with open interior, and smooth external boundary $\partial\mathcal{M}$. Its interior is then further subdivided into a finite number of non-interpenetrating regions, with the union of all internal and external boundaries denoted by Σ. The planet's gravitational potential ϕ satisfies the Poisson equation

$$\nabla^2\phi = 4\pi G\varrho\,, \tag{1}$$

which is to hold within $\mathbb{R}^3$, where ϱ is the density, G the universal gravitational constant and ∇^2 the Laplacian operator; the density is non-zero only in $\mathcal{M}$. This equation is solved subject to the boundary and regularity conditions

(i) $[\phi]^+_- = [\langle\hat{\mathbf{n}}, \nabla\phi\rangle]^+_- = 0$ for $\mathbf{x} \in \Sigma$,
(ii) $\phi \to 0$ as $\|\mathbf{x}\| \to \infty$,

where $\hat{\mathbf{n}}$ is the outward unit normal vector to a boundary, $[\cdot]^+_-$ denotes the jump in a quantity across the boundary in the direction of $\hat{\mathbf{n}}$, ∇ is the gradient operator, $\langle\cdot,\cdot\rangle$ denotes the standard inner product on $\mathbb{R}^3$, and $\|\cdot\|$ is the associated norm.

2.2 Weak form of Poisson's equation

Following Chaljub & Valette (2004), we will express the problem in weak form on a bounded domain through the use of an appropriate DtN map. Let $\mathcal{B} = \{\mathbf{x} \in \mathbb{R}^3 \mid \|\mathbf{x}\| \leq b\}$ denote a closed ball of radius b which contains $\mathcal{M}$, and ψ be a sufficiently regular complex-valued function defined on $\mathcal{B}$. We multiply eq. (1) by the complex-conjugate $\overline{\psi}$ of this test function and integrate to obtain

$$\int_{\mathcal{B}} (\nabla^2 \phi)\overline{\psi}\, d^3\mathbf{x} = 4\pi G \int_{\mathcal{M}} \varrho\, \overline{\psi}\, d^3\mathbf{x}\,. \tag{2}$$

The use of complex-valued functions is to facilitate our later introduction of spherical harmonic expansions. Integrating the left hand side of eq. (2) by parts we arrive at

$$\int_{\mathcal{B}} \left\langle \nabla\phi, \nabla\overline{\psi} \right\rangle d^3\mathbf{x} - \int_{\partial\mathcal{B}} \langle \hat{\mathbf{n}}, \nabla\phi \rangle\, \overline{\psi}\, dS = -4\pi G \int_{\mathcal{M}} \varrho\, \overline{\psi}\, d^3\mathbf{x}\,, \tag{3}$$

where we have used the continuity conditions on ϕ and its normal derivative across Σ. To account for the term $\langle \hat{\mathbf{n}}, \nabla\phi \rangle$ within the surface integral over $\partial\mathcal{B}$ we use the fact that ϕ is harmonic in $\mathbb{R}^3 \setminus \mathcal{B}$. It follows that the value of ϕ within this exterior domain is determined uniquely by its restriction to $\partial\mathcal{B}$, and we have, in particular, the well-known expansion

$$\phi(r, \theta, \varphi) = \sum_{lm} \left(\frac{b}{r}\right)^{l+1} \phi_{lm}(b) Y^0_{lm}(\theta, \varphi)\,. \tag{4}$$

valid for $r \geq b$, where Y^N_{lm} denote the fully normalized GSPHs of degree l, order m, and upper index N (e.g. Dahlen & Tromp 1998). Here the expansion coefficients of the restriction of the potential to $\partial\mathcal{B}$ are given by the integrals

$$\phi_{lm}(b) = \int_{\mathbb{S}^2} \phi(b, \theta, \varphi)\overline{Y^0_{lm}(\theta, \varphi)}\, dS, \tag{5}$$

where $\mathbb{S}^2$ is the unit two-sphere. Using this result, we find that

$$\langle \hat{\mathbf{n}}, \phi \rangle|_{\partial\mathcal{B}} = -\sum_{lm} \frac{l+1}{b} \phi_{lm}(b) Y^0_{lm}(\theta, \varphi), \tag{6}$$

and hence eq. (3) can be written

$$\int_{\mathcal{B}} \left\langle \nabla\phi, \nabla\overline{\psi} \right\rangle d^3\mathbf{x} + \sum_{lm} (l+1) b\, \phi_{lm}(b)\, \overline{\psi_{lm}(b)} = -4\pi G \int_{\mathcal{M}} \varrho\, \overline{\psi}\, d^3\mathbf{x}\,, \tag{7}$$

which is to hold for all test functions ψ. This is the desired weak form of the problem. Importantly, the role of the exterior potential has been reduced to non-local boundary terms involving its spherical harmonic expansion coefficients on $\partial\mathcal{B}$.

2.3 Transformation of Poisson's equation

The weak form of Poisson's equation in eq. (7) provides a suitable starting point for numerical discretization using, for example, a 3-D spectral element method (e.g. Chaljub & Valette 2004). However, we cannot use methods based upon GSPH expansions to tackle this problem if the planet is not geometrically spherical because the continuity conditions on ϕ across the boundaries Σ cannot be readily enforced. In order to apply such an approach we must transform the problem into an equivalent one defined on a geometrically spherical domain.

Consider a diffeomorphism $\boldsymbol{\xi} : \mathcal{B} \to \mathcal{B}$ (i.e. a smooth mapping, with a smooth inverse) with the following properties:

(i) its restriction to the boundary $\partial\mathcal{B}$ is the identity mapping;
(ii) the inverse image $\tilde{\mathcal{M}} = \boldsymbol{\xi}^{-1}(\mathcal{M})$ is a ball with centre coincident with that of $\mathcal{B}$;
(iii) the inverse image $\tilde{\Sigma} = \boldsymbol{\xi}^{-1}(\Sigma)$ of the boundary set is comprised of concentric spheres in $\tilde{\mathcal{M}}$.

For general $\mathcal{M}$ such a diffeomorphism will not exist, and so we see the fundamental restriction of our method. Nonetheless, for many applications a suitable diffeomorphism can be found, and later we discuss how this can be done practically. In fact, the requirement that this mapping be smooth is more stringent than is strictly necessary, and it is possible for it to be defined in a piecewise manner with continuity enforced at interfaces.

Using this diffeomorphism, we can define a new *referential potential field*

$$\zeta(\mathbf{x}) = (\phi \circ \boldsymbol{\xi})(\mathbf{x}) := \phi[\boldsymbol{\xi}(\mathbf{x})], \tag{8}$$

where $\circ$ denotes the composition of two functions. Knowledge of ζ is equivalent to that of ϕ, but ζ is defined on a geometrically spherical domain. Our first aim is to show that ζ satisfies a suitably generalized form of Poisson's equation. Using $\boldsymbol{\xi}$ to change variables in eq. (7), we arrive at

$$\int_{\mathcal{B}} J \left\langle \mathbf{F}^{-T}\nabla\zeta, \mathbf{F}^{-T}\nabla\overline{\chi} \right\rangle d^3\mathbf{x} + \sum_{lm} (l+1) b\, \zeta_{lm}(b)\, \overline{\chi_{lm}(b)} = -4\pi G \int_{\tilde{\mathcal{M}}} J\varrho \circ \boldsymbol{\xi}\, \overline{\chi}\, d^3\mathbf{x}\,. \tag{9}$$

where we have defined a new test function $\chi = \psi \circ \boldsymbol{\xi}$, along with the *deformation gradient* $\mathbf{F}$ of the diffeomorphism, which has components

$$[\mathbf{F}]_{ij} \equiv \frac{\partial \xi_i}{\partial x_j}\,, \tag{10}$$

and its *Jacobian*,

$$J = \det \mathbf{F}\,, \tag{11}$$

which we assume without loss of generality to be everywhere positive. We have also applied the chain rule to arrive at the identity

$$(\nabla \phi) \circ \boldsymbol{\xi} = \mathbf{F}^{-T} \nabla \zeta, \tag{12}$$

along with a corresponding expression involving the gradients of the test functions. At this stage it is convenient to define the *right Cauchy–Green deformation tensor*,

$$\mathbf{C} = \mathbf{F}^T \mathbf{F}\,, \tag{13}$$

a tensor derived from it,

$$\boldsymbol{a} = J\mathbf{C}^{-1}\,, \tag{14}$$

and the *referential density*,

$$\rho = J\varrho \circ \boldsymbol{\xi}\,. \tag{15}$$

With these definitions, the transformed weak form for ζ can be written

$$\int_{\mathcal{B}} \langle \mathbf{a}\, \nabla\zeta, \nabla\overline{\chi} \rangle \; d^3\mathbf{x} + \sum_{lm} (l+1) b\, \zeta_{lm}(b)\, \overline{\chi_{lm}(b)} = -4\pi G \int_{\tilde{\mathcal{M}}} \rho\, \overline{\chi}\, d^3\mathbf{x}\,, \tag{16}$$

which is to hold for all test functions χ. This equation broadly resembles the original weak formulation, but involves the tensor field $\mathbf{a}$ determined from the diffeomorphism $\boldsymbol{\xi}$. By construction, these problems are mathematically equivalent: in essence we have just exchanged simplicity of the equation for simplicity of the domain in which it is posed. From a numerical perspective, however, it is only in the transformed problem that we can usefully apply methods based on GSPH expansions.

3 NUMERICAL IMPLEMENTATION

3.1 Numerical discretization of the problem

Our approach to solving eq. (16) numerically is based on GSPH expansions for the angular dependence of the referential potential, along with a spectral-element discretization in the radial co-ordinate. Within $\mathcal{B}$, the truncated GSPH expansion of the referential potential takes the form

$$\zeta(r,\theta,\varphi) = \sum_{l=0}^{L} \sum_{m=-l}^{l} \zeta_{lm}(r) Y_{lm}^0(\theta,\varphi)\,, \tag{17}$$

where the maximum expansion degree L is to be chosen based on the planet's structure and properties. Each of the radial expansion coefficients ζ_{lm} is then expanded in a finite set of radial basis functions

$$\zeta_{lm}(r) = \sum_{n=1}^{N} \zeta_{lmn} h_n(r). \tag{18}$$

The specific basis functions used are Lagrange polynomials defined on a radial spectral element mesh (e.g. Komatitsch & Tromp 1999; Al-Attar & Tromp 2014). Importantly, the radial mesh is built to honour the discontinuities within the reference planet $\tilde{\mathcal{M}}$, and thus we can enforce the required continuity of ζ in a trivial manner. The appropriate continuity conditions on the gradient of the referential potential are built directly into the weak formulation of the problem, and so need not be considered explicitly.

The test functions for the problem are taken in turn to be $\chi = h_n Y_{lm}^0$ as the indices l, m and n range over appropriate values, and in this manner we arrive at a system of linear equations

$$Ax = f, \tag{19}$$

where the vector x contains the expansion coefficients ζ_{lmn}, while the matrix A and force vector f are obtained through discretization of the weak form in a manner detailed below. Specifically, we represent x by defining for each l and m an N-component vector x_{lm} the n'th component of which is ζ_{lmn},

$$[x_{lm}]_n = \zeta_{lmn}\,. \tag{20}$$

All the x_{lm} are then bundled together into the $[N(L+1)^2]$-component column-vector

$$x = \begin{pmatrix} x_{00} \\ x_{1-1} \\ x_{10} \\ \vdots \\ x_{lm} \\ \vdots \\ x_{LL} \end{pmatrix}, \tag{21}$$

and the components of the force, f_{lmn} (computed below), are arranged similarly. Importantly, explicit calculation of the components of A, which can be large, is not required. Instead, we need only ever compute its action on a given vector as part of the iterative solution of the linear system.

3.2 Hybrid pseudospectral/spectral element calculations

To determine the action of the matrix A and to compute the force vector f, we use a hybrid pseudospectral/spectral element method similar to that of Crawford (2018) for modelling glacial isostatic adjustment in the presence of laterally varying mantle viscosity. This approach also closely resembles the method of Leng *et al.* (2016) and Leng *et al.* (2019) for modelling global seismic wave propagation, though in their work a 2-D spectral element method is coupled to a Fourier-series expansion in an azimuthal variable about the source location.

To explain the key ideas, we start with the computation of the force vector, which is part of the preprocessing for the potential calculation. The components f_{lmn}, having been computed once, are stored and used at the first stage of the iterative solution. The (l, m, n)th element of the force vector is given by the integral

$$f_{lmn} = -4\pi G \int_{\tilde{\mathcal{M}}} \rho\, h_n\, \overline{Y^0_{lm}}\, d^3\mathbf{x}, \tag{22}$$

where we note that the radial basis functions are real valued. Using spherical polar co-ordinates the volume integral can be reduced to

$$\int_{\tilde{\mathcal{M}}} \rho\, h_n\, \overline{Y^0_{lm}}\, d^3\mathbf{x} = \int_0^a \rho_{lm}\, h_n\, r^2\, dr, \tag{23}$$

where ρ_{lm} is the (l, m)th GSPH coefficient of the referential density and a denotes the radius of the reference planet $\tilde{\mathcal{M}}$; once ρ_{lm} is known, the radial integral can be evaluated using the numerical quadrature formula associated with the spectral element discretization. How we find ρ_{lm} depends on the way in which the planet's structure is specified. On the one hand, the density might be described referentially, with ρ and $\boldsymbol{\xi}$ given, in which case we obtain ρ_{lm} by applying a fast GSPH transformation at each radial node to calculate the GSPH coefficients for an appropriate range of indices. In detail, this transformation is done using Gauss-Legendre quadrature in colatitude coupled to a fast Fourier transformation in longitude (*cf.* Lognonné & Romanowicz 1990). On the other hand, if the model is specified by the *physical* density $\varrho(\mathbf{x})$ then we must first determine $\rho(\mathbf{x})$. To do this, we use eq. (15) to determine the values of ρ on an appropriate spatial grid and then proceed as before.

Turning to the action of the matrix A, suppose we wish to determine Ax, with x defined as above to contain the components of the discretized referential gravitational potential ζ. It will be useful to define an auxiliary vector field

$$\mathbf{q} = \mathbf{a}\nabla\zeta, \tag{24}$$

where we recall that $\mathbf{a}$ is the symmetric tensor field introduced in eq. (14). Working in the canonical basis of Phinney & Burridge (1973) (see Appendix A) the components of this vector field can be expanded as

$$q^\alpha = \sum_{lm} q^\alpha_{lm} Y^\alpha_{lm}. \tag{25}$$

Taking the (l, m, n)th test function, we can apply the rules for contravariant differentiation (e.g. Dahlen & Tromp 1998, Appendix C) to reduce the left-hand side of eq. (16) to

$$\int_0^b \left[r^2 h_n' q^0_{lm} + \frac{k}{\sqrt{2}} r h_n \left(q^+_{lm} + q^-_{lm} \right) \right] dr + b(l+1) h_n(b) \zeta_{lm}(b), \tag{26}$$

where $k = \sqrt{l(l+1)}$. Assuming we know the functions q^α_{lm}, the radial integral can be trivially evaluated using numerical quadrature, and gives the desired element of Ax.

Calculation of the coefficient functions q^α_{lm} is done in a number of stages, following the standard pseudospectral philosophy by which we work in either the spatial or spectral domain based on what is simplest (e.g. Boyd 2001). Starting from the expansion coefficient functions ζ_{lm}, we use the rules for contravariant differentiation along with those for Lagrange polynomial interpolation to determine $\zeta^{|\alpha}_{lm}$, the expansion coefficients of $\nabla\zeta$ relative to the canonical basis. Inverse fast GSPH transformations are then performed to find the values of $\nabla\zeta$ on a spatial

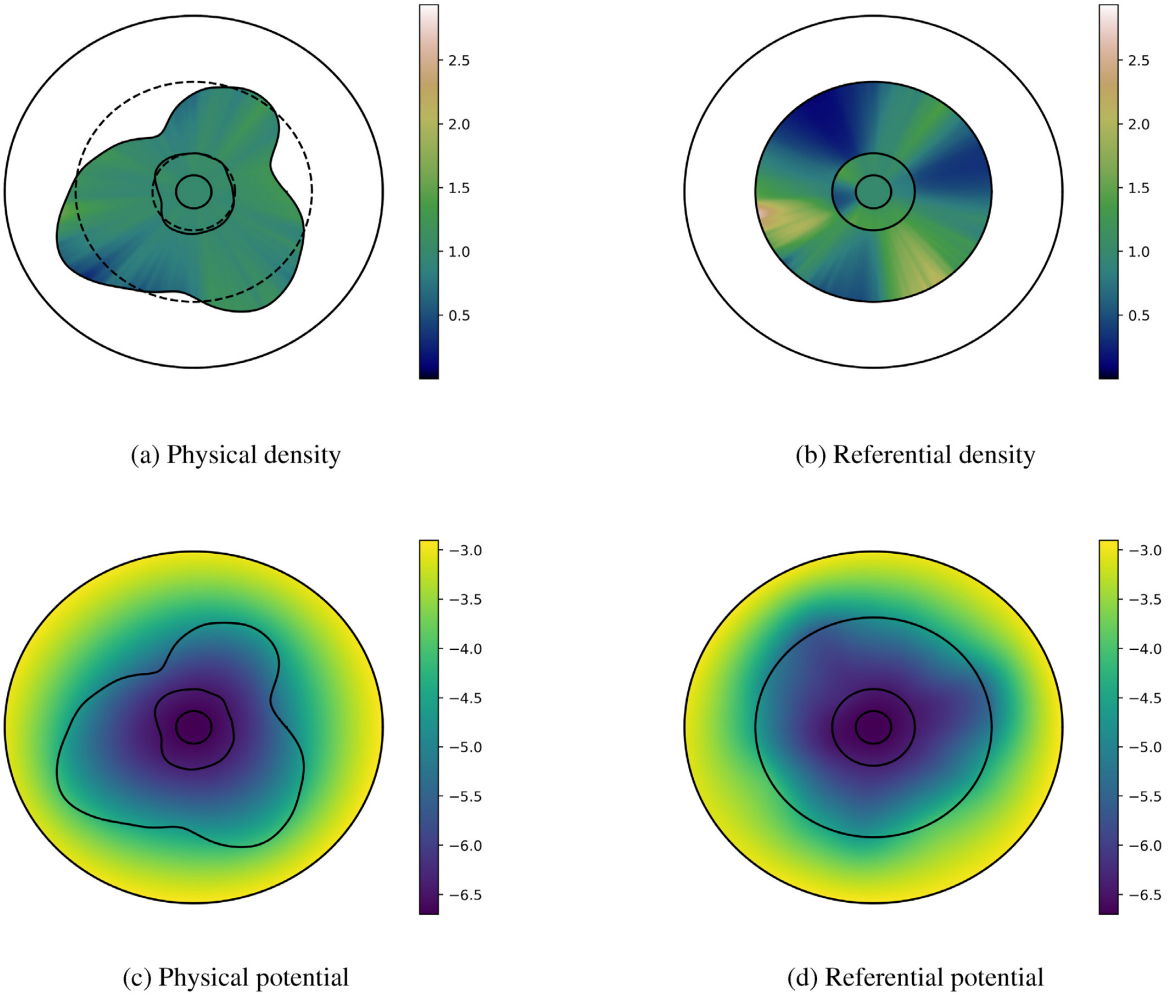

(a) Physical density

(b) Referential density

(c) Physical potential

(d) Referential potential

Figure 1. The stages in the calculation of ϕ for an aspherical, layered planet. Each panel shows a slice through the plane $\theta = \pi/2$, and a small, homogeneous sphere has been placed around the origin in order to ensure that $\boldsymbol{\xi}$ and ρ are both regular at the origin. Panel (a) shows the planet before performing any transformations. In panel (b) the computational domain $\mathcal{B}$ has been transformed through the action of $\boldsymbol{\xi}$: the boundaries of the planet are spherical and the density has been transformed accordingly. Panel (d) shows ζ, the solution to eq. (16). Moving left from (d) to (c) the planet and potential are mapped from reference space back to physical space, yielding the potential ϕ.

mesh. Multiplication by $\mathbf{a}$ is performed spatially to obtain $\mathbf{q} = \mathbf{a}\nabla\zeta$ on this grid, and finally the required coefficient functions q^{α}_{lm} are obtained through forward fast GSPH transformations. Within this process forward and inverse fast GSPH transformations must—potentially—be performed at each node of the radial mesh, and this accounts for a substantial part of our method's computational cost. Importantly, however, in regions where the diffeomorphism is the identity we have $\mathbf{a}(\mathbf{x}) = \mathbf{1}$, so these transformations are not needed and we can make substantial computational savings.

3.3 Pre-conditioned iterative solution of the linear system

The numerical solution of eq. (19) is accomplished most efficiently using matrix-free iterative methods. From eq. (16) it is clear that A is an Hermitian matrix, and so we can apply the pre-conditioned conjugate gradient algorithm (e.g. Saad 2003). In order for this algorithm to converge rapidly a good pre-conditioner B for the linear system must be found. Here a balance must be struck between B being a good approximation to the inverse operator A^{-1}—meaning the algorithm will converge in fewer iterations—and the cost of determining the action of B. The preconditioner which we have used in all our numerical examples is

$$B = \left(A^{(0)}\right)^{-1}, \tag{27}$$

where $A^{(0)}$ is the system matrix for the corresponding spherical system, that is the matrix obtained by considering eq. (16) with $\boldsymbol{\xi}(\mathbf{x}) = \mathbf{x}$.

The reasoning behind this choice is similar to that of Al-Attar *et al.* (2012) in the context of normal mode coupling calculations. One starts by observing that when the planet is geometrically spherical there is a complete decoupling between the coefficients for different spherical harmonic degrees and orders, which gives the corresponding matrix $A^{(0)}$ a block diagonal structure. The matrix $A^{(0)}_l$ associated with

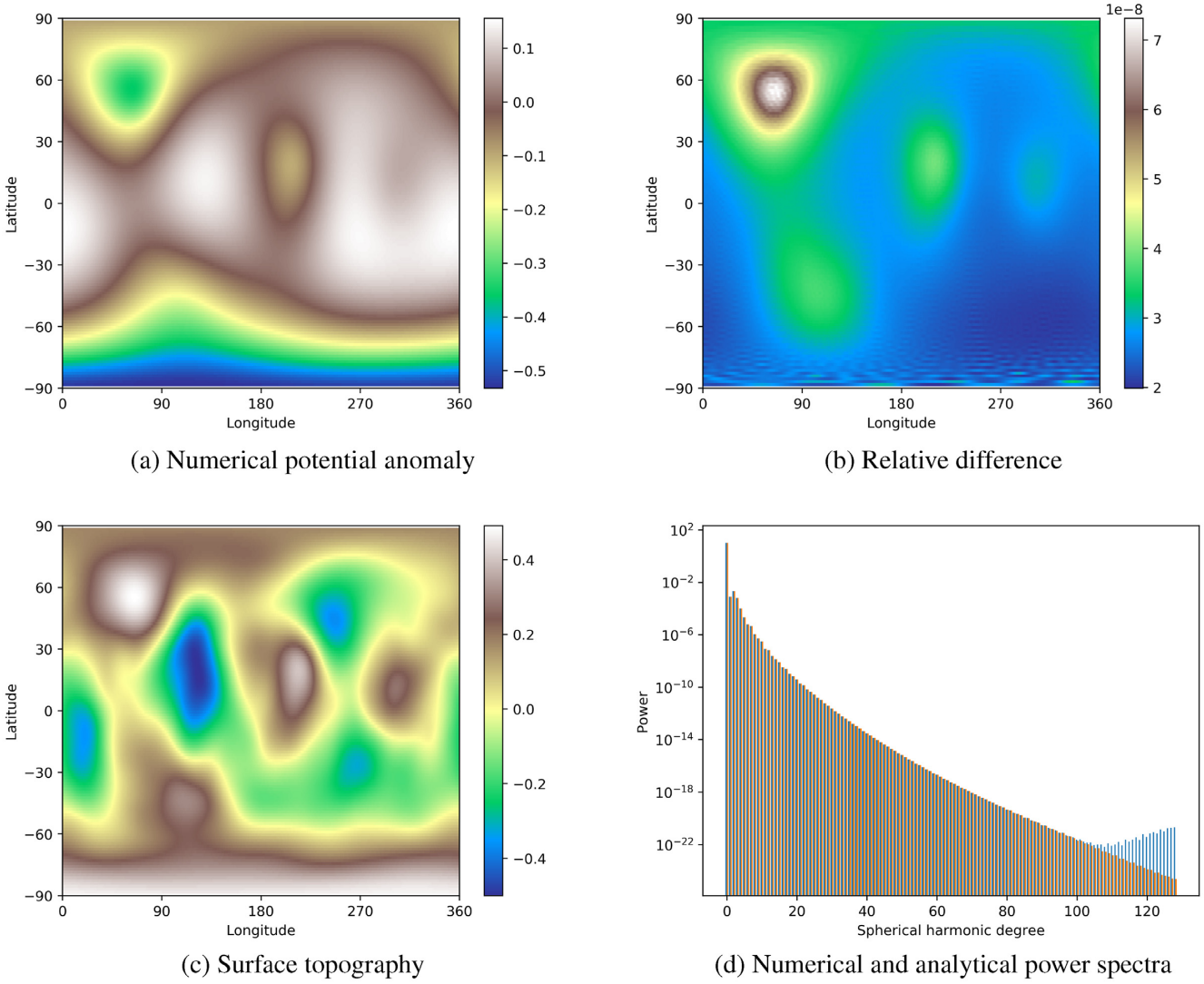

Figure 2. The potential and topography of the body considered in Fig. 1, evaluated on $\partial\mathcal{B}$. Panel (a) shows the numerical potential anomaly. Long-wavelength features of the topography—shown in panel (c)—are clearly visible. In panel (d) we have plotted the numerical (blue) and analytical (red) values of the normalized power-spectra, P_l. There is excellent agreement until about $l = 100$. Thereafter, the two spectra deviate somewhat, but the power at these higher degrees is so small that the spatial field is not affected noticeably. Indeed, the relative difference between the numerical and analytical fields, normalized by the maximum absolute value of the analytical field, is only a few parts in 10^8, as shown in panel (b).

the (l, m)th subsystem is independent of m, and can be readily computed in terms of the radial spectral element discretization (*cf.* Al-Attar & Tromp 2014, Appendix D2). Moreover, the matrices $A_l^{(0)}$ for each l are Hermitian and narrow banded, meaning that their LU-decomposition can be computed and stored in an efficient manner using standard LAPACK routines for banded matrices. Once these factorizations have been performed, the action of $\left(A^{(0)}\right)^{-1}$ can be computed rapidly by carrying out $(L+1)^2$ simple backsubstitutions. The action of the block-diagonal pre-conditioner on the vector f can then be written

$$\left(A^0\right)^{-1} f = \begin{pmatrix} \left(A_0^{(0)}\right)^{-1} f_{00} \\ \left(A_1^{(0)}\right)^{-1} f_{1-1} \\ \left(A_1^{(0)}\right)^{-1} f_{10} \\ \vdots \\ \left(A_l^{(0)}\right)^{-1} f_{lm} \\ \vdots \\ \left(A_L^{(0)}\right)^{-1} f_{LL} \end{pmatrix}. \tag{28}$$

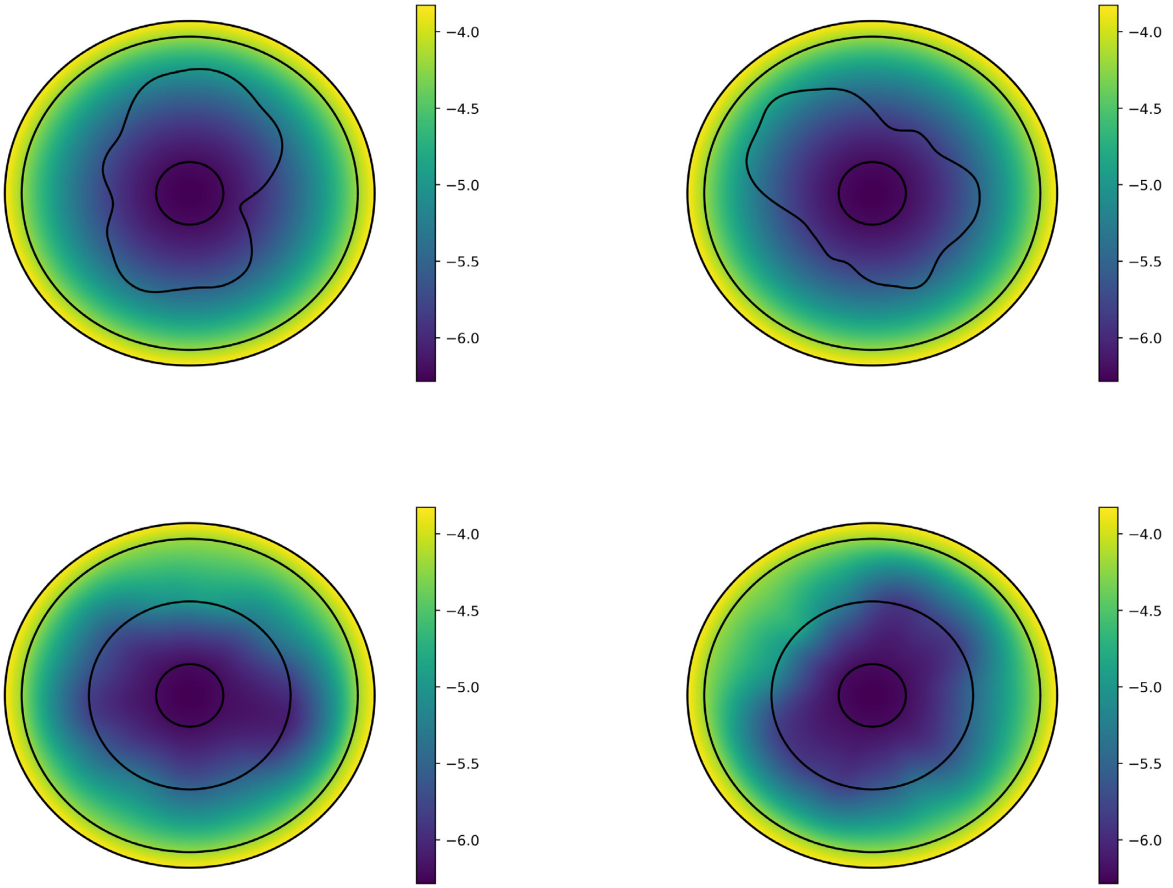

Figure 3. A comparison of the referential and physical potentials of two 'different' homogeneous spheres, each containing a different internal 'boundary' with large topography. The bottom two panels show the referential potentials which, being the result of applying different mappings to $\mathcal{B}$, are not the same. By contrast, the physical potentials, shown above, agree to numerical precision.

Not only is the action of $\left(A^{(0)}\right)^{-1}$ cheap to compute, but we also expect that $A^{(0)}$ will approximate A reasonably well for a body which is nearly spherical, with the approximation improving as $\mathcal{M}$ approaches geometrical sphericity. This suggests that $\left(A^{(0)}\right)^{-1}$ should act as a good preconditioner in a moderately aspherical system, and this is borne out by later numerical examples.

Within Al-Attar *et al.* (2012) it was found that for normal mode calculations such a 'spherical earth pre-conditioner' could usually be out-performed by allowing some limited coupling between the off-diagonal subblocks. We have not investigated that for the present problem, but it might be worth considering in future work if applications to very aspherical planets are necessary (see Section 5).

4 NUMERICAL EXAMPLES AND BENCHMARKS

4.1 The form of $\boldsymbol{\xi}$

Finding a diffeomorphism which maps an aspherical, multilayered planet onto a geometrically spherical reference body is a problem in its own right. Therefore, for the rest of this work we restrict attention to mappings of the form

$$\boldsymbol{\xi}(\mathbf{x}) = \mathbf{x} + h(\mathbf{x})\hat{\mathbf{x}}\,, \tag{29}$$

where h is a scalar-valued function. Physically, $\boldsymbol{\xi}$ causes displacement along *radial* lines: hence, we shall describe these mappings as 'radial'. This choice of $\boldsymbol{\xi}$ limits our scope somewhat, but despite its apparent simplicity we can still study a broad class of planetary bodies. We emphasize, though, that the method described above is applicable, in principle, to any body that can be mapped diffeomorphically onto a ball.

For mappings of the form of eq. (29), we show in Appendix B that its Jacobian is

$$J = \left(1 + \frac{h}{r}\right)^2 (1 + \partial_r h)\,. \tag{30}$$

In order for $\boldsymbol{\xi}$ to be a diffeomorphism it is necessary for J to be everywhere positive, so the form of h is restricted; we emphasize, however, that this function is not required to be small in any sense.

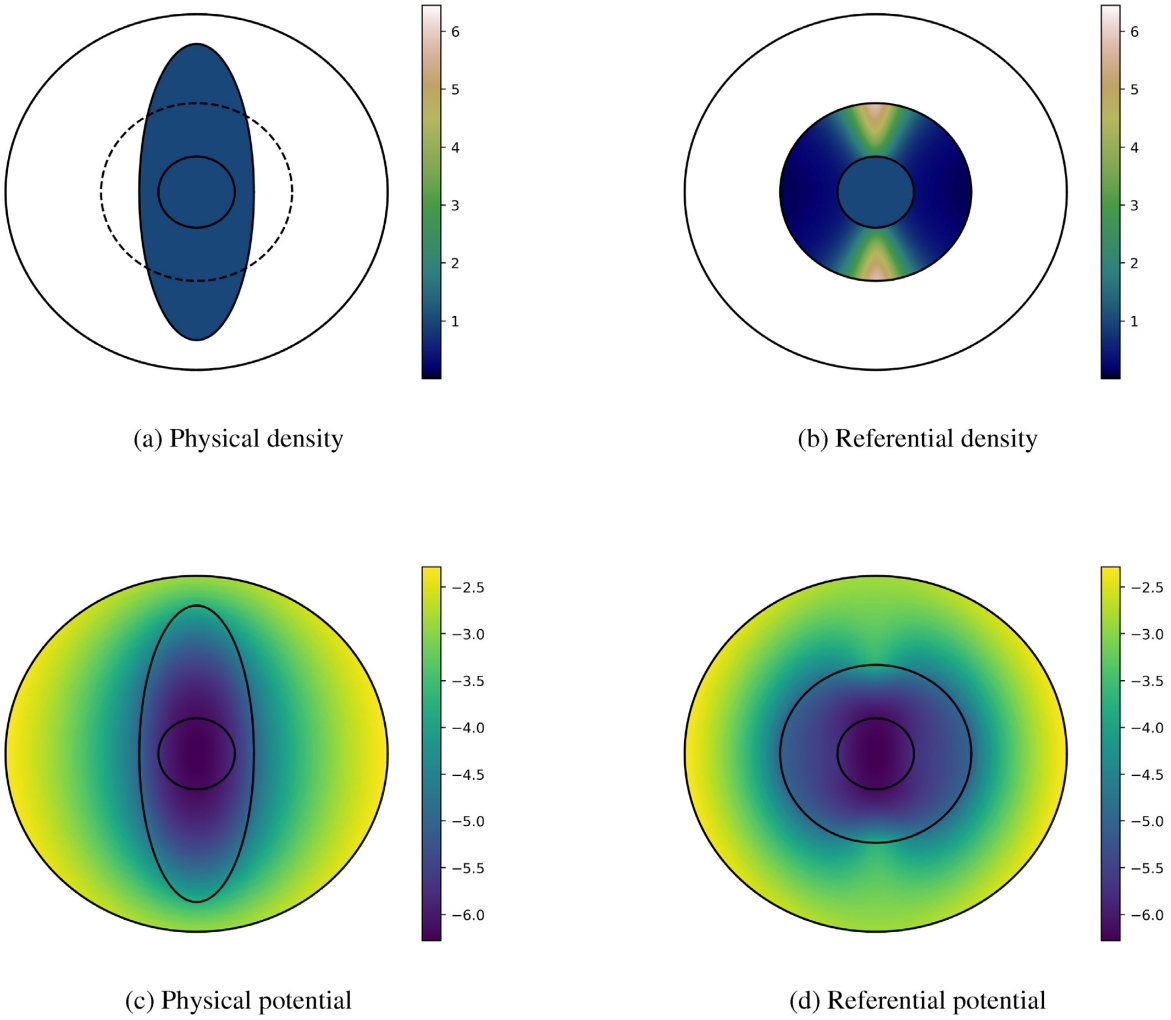

Figure 4. An illustration of the numerical method for a highly flattened ellipsoid. The body is homogeneous, which clarifies the mapping procedure visually. See Fig. 1 for a description of the stages.

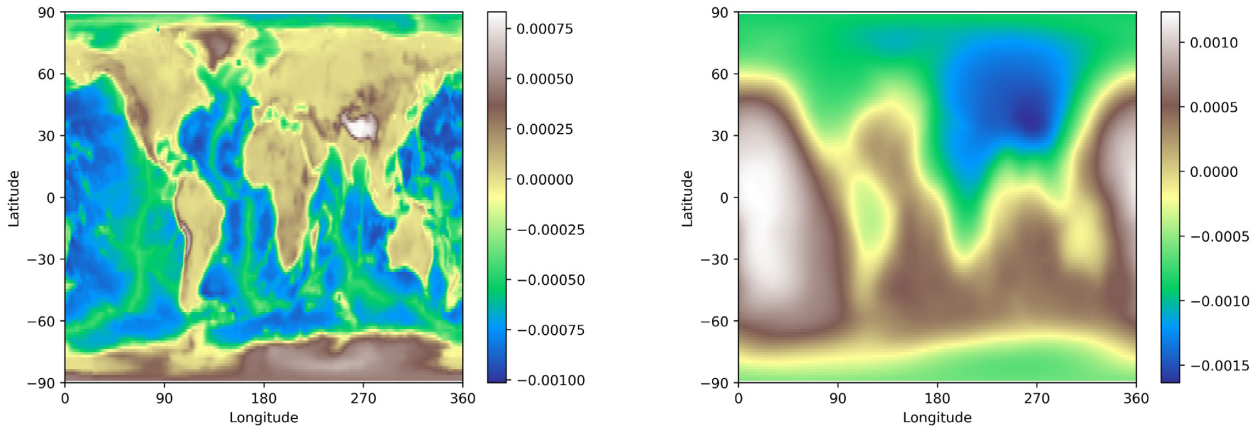

Figure 5. A homogeneous body with Terran topography, with the computation performed accurate to maximum degree $L = 128$. The left-hand panel shows the topography. On the top right is plotted the potential anomaly at a radius of 1.05, corresponding to an actual altitude of about 300 km.

In practice, we generate h by specifying the desired topography on each reference boundary and smoothly interpolating between them. In detail, the topography on the i'th reference boundary is defined to be h_i, with the boundary being a sphere of radius R_i, and we demand that $h|_{r=R_i} = h_i$. Since it is permissible that $\boldsymbol{\xi}$ be only piecewise-smooth and continuous across referential boundaries, hence we are free, if desired, to interpolate the form of h within each layer separately, while only enforcing continuity at the boundary radii. Once h has been specified throughout $\mathcal{B}$ we can calculate and store $a^{\alpha\beta}$, the contravariant components of $\mathbf{a}$ with respect to the canonical basis (see Appendix B for details).

4.2 Tests, benchmarks and illustrations

In this section we present some examples and test the accuracy of our method. All physical quantities are presented non-dimensionalized, with

(i) density scaled by $\tilde{\varrho} = 5150\,\mathrm{kg\,m^{-3}}$, Earth's average density,
(ii) length scaled by $\tilde{L} = 6.371 \times 10^6\,\mathrm{m}$, the average radius of the Earth,
(iii) potential itself scaled by $\tilde{\phi} = G\tilde{\varrho}\tilde{L}^2$.

4.2.1 Comparison with semi-analytical solution

In order to test the numerical method we must compare its results with those obtained from semi-analytical calculations. Therefore we consider the case of a planet composed of N_L layers, each layer having arbitrary topography on its surface subject to the constraint that the boundaries between the layers not interpenetrate. Furthermore, within the i'th layer the density is parametrized as a polynomial of degree N_p with laterally varying coefficients,

$$\varrho_i(r,\theta,\varphi) = \sum_{j=1}^{N_p} \varrho_i^{(j)}(\theta,\varphi)\, r^j \,. \tag{31}$$

Generalizing the results of Balmino (1994), the potential on a spherical surface which encloses the planet can be written analytically as a sum over the planet's layers and over spherical harmonic degrees and polynomial orders. The potential at a point $\mathbf{x}$, inside or outside the body, is of course

$$\phi(\mathbf{x}) = -G \int_{\mathcal{M}} \frac{\varrho(\mathbf{x}')}{\|\mathbf{x}-\mathbf{x}'\|} d\mathbf{x}' \,. \tag{32}$$

Let b be the radius of a sphere which completely bounds the body. If $\|\mathbf{x}\| \geq b$, then we may expand the above integral using the identity

$$\frac{1}{\|\mathbf{x}-\mathbf{x}'\|} = \frac{1}{r} \sum_{lm} \frac{4\pi}{2l+1} \left(\frac{r'}{r}\right)^l \overline{Y_{lm}^0(\theta',\varphi')}\, Y_{lm}^0(\theta,\varphi) \,, \tag{33}$$

from Dahlen & Tromp (1998, Appendix B). A simple calculation then shows that the (l, m)th component of the potential on the spherical surface $r = b$ is given by

$$\phi_{lm}(b) = -\frac{4\pi G}{(2l+1)b^{l+1}} \left\{ \sum_{i=1}^{N_L} \sum_{j=0}^{N_p} \frac{[R_i + h_i(\theta,\varphi)]^{l+N_p+j} \left[\varrho_i^{(j)}(\theta,\varphi) - \varrho_{i+1}^{(j)}(\theta,\varphi)\right]}{l+N_p+j} \right\}_{lm} , \tag{34}$$

where $\varrho_{N_L+1}^{(j)}$ is defined to vanish identically for all j.

For the body considered in Fig. 1 we have plotted in Fig. 2 the numerical potential anomaly,

$$\phi_\mathrm{anom}(r,\theta,\varphi) = \phi(r,\theta,\varphi) - \phi_{00}(r) \,, \tag{35}$$

the normalized difference between the numerical and analytical potentials, and the respective normalized power-spectra,

$$P_l(r) = \frac{\sum_m |\phi_{lm}(r)|^2}{|\phi_{00}(r)|^2} \,, \tag{36}$$

on $\partial\mathcal{B}$, corresponding to a radius of $r = 1.6$. The surface topography is also shown for reference. We see from panel (d) that the numerical and analytical potentials agree closely, having identical power-spectra up to around $l = 100$. Although the power-spectra differ beyond that degree, the potential has so little power in those higher degrees that the spatial field is not affected appreciably.

The difference between the power-spectra at high degrees is due to truncation. If the planet were homogeneous with small topography, then the potential would have the same maximum degree as the topography. However, the nonlinear interactions between large topography and heterogeneous density produce a potential with power at all degrees. By truncating the spherical-harmonic expansion we necessarily neglect some of this behaviour. Therefore, the maximum spherical-harmonic degree required to calculate ϕ to a given level of accuracy will not just be the larger of the maximum degree in the density and topography. Rather, it must be chosen based on the roughness of the referential density ρ and the tensor field $\mathbf{a}$. While this issue has not been investigated fully, we can easily check for convergence in each instance by repeating calculations at increasing maximum degrees.

4.2.2 Independence of the form of $\boldsymbol{\xi}$

A physical planet can be represented by many different reference bodies, each with its own diffeomorphism and associated referential density. Our numerical method must, of course, be independent of the arbitrary choice of diffeomorphism. To verify this, we consider a homogeneous, spherical planet along with two distinct referential descriptions as illustrated in Fig. 3. Whilst the respective referential potentials are clearly different, we see that they map to the same physical potential.

4.3 Further examples

Having shown that our method gives numerically accurate answers we conclude by showing two more illustrative example calculations. First, in Fig. 4 we show the calculated potential of a highly flattened, homogeneous ellipsoid. Calculations of this type are required in determining hydrostatic equilibrium figures of rapidly rotating planets, this being a potential future application of this work.

Finally, Fig. 5 shows the potential of a homogeneous body with the Earth's topography expanded up to degree 128. While the topography contains relatively short wavelengths, it is only of a very low amplitude compared to the Earth's radius. We can, therefore, chose the diffeomorphism to equal the identity mapping everywhere but a thin spherical annulus enclosing the surface. As discussed earlier, this greatly increases the speed of the calculations.

5 DISCUSSION

We have presented a new method for performing numerically exact calculations of the gravitational potential of aspherical and heterogeneous planets. The novel feature of this work is the use of a diffeomorphism $\boldsymbol{\xi}$ to map $\mathcal{M}$, a heterogeneous planet with arbitrarily large topography, onto $\tilde{\mathcal{M}}$, a geometrically spherical reference body in which pseudospectral methods can be used in conjunction with 1-D spectral element methods. The numerical examples demonstrate that the method is accurate, has an efficiency that scales with the planet's complexity, and can even be applied to markedly aspherical planets. It is worth noting that all of these examples were run on a desktop computer, and do not require the use of parallel computations.

The chief motivation behind our work is the desire to perform elastodynamics calculations in aspherical planets efficiently without approximating the effects of self-gravity and topography. In this context, the geometric transformations we have used can be interpreted physically as 'particle-relabelling transformations' as described by Al-Attar & Crawford (2016) and Al-Attar *et al.* (2018). The necessary extensions will be described in future work, with application to hydrostatic equilibrium figures, free-oscillation seismology, body tides, and rotational dynamics. Furthermore, there are bodies of interest in the planetary sciences which, although diffeomorphic to a ball, cannot be described using the radial mappings currently implemented. A particularly salient example are the 'synestias' introduced by Lock & Stewart (2017). An important extension of this work, then, is to investigate the efficient generation of more general diffeomorphisms.

ACKNOWLEDGEMENTS

MM is supported by an EPSRC studentship and a CASE award from BP. We thank John Woodhouse for providing a new routine for efficient computation of generalized Legendre functions. We are grateful to Frédéric Chambat, an anonymous reviewer and editor Gaël Choblet for their helpful comments and suggestions.

REFERENCES

Al-Attar, D. & Crawford, O., 2016. Particle relabelling transformations in elastodynamics, *Geophys. J. Int.,* **205**(1), 575–593.

Al-Attar, D. & Tromp, J., 2014. Sensitivity kernels for viscoelastic loading based on adjoint methods, *Geophys. J. Int.,* **196**(1), 34–77.

Al-Attar, D., Woodhouse, J.H. & Deuss, A., 2012. Calculation of normal mode spectra in laterally heterogeneous earth models using an iterative direct solution method, *Geophys. J. Int.,* **189**(2), 1038–1046.

Al-Attar, D., Crawford, O., Valentine, A.P. & Trampert, J., 2018. Hamilton's principle and normal mode coupling in an aspherical planet with a fluid core, *Geophys. J. Int.,* **214**(1), 485–507.

Balmino, G., 1994. Gravitational potential harmonics from the shape of an homogeneous body, *Celest. Mech. Dyn. Astron.,* **60**(3), 331–364.

Barnett, C.T., 1976. Theoretical modeling of the magnetic and gravitational fields of an arbitrarily shaped threedimensional body, *Geophysics,* **41**(6), 1353–1364.

Beer, G. & Meek, J.L., 1981. "infinite domain" elements, *Int. J. Numer. Methods Eng.,* **17**(1), 43–52.

Bettess, P., 1977. Infinite elements, *Int. J. Numer. Methods Eng.,* **11**(1), 53–64.

Boyd, J.P., 2001. *Chebyshev and Fourier Spectral Methods,* Courier Corporation.

Chaljub, E. & Valette, B., 2004. Spectral element modelling of three-dimensional wave propagation in a self-gravitating earth with an arbitrarily stratified outer core, *Geophys. J. Int.,* **158**(1), 131–141.

Chambat, F. & Valette, B., 2005. Earth gravity up to second order in topography and density, *Phys. Earth planet. Inter.,* **151**(1-2), 89–106.

Chambat, F., Ricard, Y. & Valette, B., 2010. Flattening of the earth: further from hydrostaticity than previously estimated, *Geophys. J. Int.,* **183**(2), 727–732.

Clairaut, A.C., 1743. *Théorie de la figure de la terre, tirée des principes de l'hydrostatique,* Paris.

Crawford, O., 2018, On the viscoelastic deformation of the Earth, *PhD thesis*, University of Cambridge.

Crawford, O., Al-Attar, D., Tromp, J. & Mitrovica, J.X., 2016. Forward and inverse modelling of post-seismic deformation, *Geophys. J. Int.,* **208**(2), 845–876.

Crawford, O., Al-Attar, D., Tromp, J., Mitrovica, J.X., Austermann, J. & Lau, H.C.P., 2018. Quantifying the sensitivity of post-glacial sea level change to laterally varying viscosity, *Geophys. J. Int.,* **214**(2), 1324–1363.

Dahlen, F. & Tromp, J., 1998. *Theoretical Global Seismology,* Princeton University Press.
Gharti, H.N. & Tromp, J., 2017. A spectral-infinite-element solution of poisson's equation: an application to self gravity, *Geophysics,* arXiv:1706.00855.
Gharti, H.N., Tromp, J. & Zampini, S., 2018. Spectral-infinite-element simulations of gravity anomalies, *Geophys. J. Int.,* **215**(2), 1098–1117.
Gharti, H.N., Langer, L. & Tromp, J., 2019. Spectral-infinite-element simulations of earthquake-induced gravity perturbations, *Geophys. J. Int.,* **217**(1), 451–468.
Hubbard, W.B., 2012. High-precision maclaurin-based models of rotating liquid planets, *Astrophys. J.,* **756**(1), L15.
Hubbard, W.B., 2013. Concentric maclaurin spheroid models of rotating liquid planets, *Astrophys. J.,* **768**(1), 43.
Jobert, N., 1976. Propagation of surface waves on an ellipsoidal earth, *Pure appl. Geophys.,* **114**(5), 797–804.
Kaula, W.M., 1964. Tidal dissipation by solid friction and the resulting orbital evolution, *Rev. Geophys.,* **2**(4), 661.
Komatitsch, D. & Tromp, J., 1999. Introduction to the spectral element method for three-dimensional seismic wave propagation, *Geophys. J. Int.,* **139**(3), 806–822.
Latychev, K., Mitrovica, J.X., Tromp, J., Tamisiea, M.E., Komatitsch, D. & Christara, C.C., 2005. Glacial isostatic adjustment on 3-d earth models: a finite-volume formulation, *Geophys. J. Int.,* **161**(2), 421–444.
Leng, K., Nissen-Meyer, T. & van Driel, M., 2016. Efficient global wave propagation adapted to 3-D structural complexity: a pseudospectral/spectral-element approach, *Geophys. J. Int.,* **207**(3), 1700–1721.
Leng, K., Nissen-Meyer, T., van Driel, M., Hosseini, K. & Al-Attar, D., 2019. Axisem3d: broadband seismic wavefields in 3-D global earth models with undulating discontinuities, *Geophys. J. Int.,* doi:10.1093/gji/ggz092
Lock, S.J. & Stewart, S.T., 2017. The structure of terrestrial bodies: Impact heating, corotation limits, and synestias, *J. geophys. Res.: Planets,* **122**(5), 950–982.
Lognonné, P. & Romanowicz, B., 1990. Modelling of coupled normal modes of the earth: the spectral method, *Geophys. J. Int.,* **102**(2), 365–395.
Martinec, Z., Pěč, K. & Burša, M., 1989. The phobos gravitational field modeled on the basis of its topography, *Earth, Moon Planets,* **45**(3), 219–235.
Medina, F. & Taylor, R.L., 1983. Finite element techniques for problems of unbounded domains, *Int. J. Numer. Methods Eng.,* **19**(8), 1209–1226.
Métivier, L., Greff-Lefftz, M. & Diament, M., 2006. Mantle lateral variations and elastogravitational deformations - I. Numerical modelling, *Geophys. J. Int.,* **167**(3), 1060–1076.
Mitrovica, J.X., Wahr, J., Matsuyama, I. & Paulson, A., 2005. The rotational stability of an ice-age earth, *Geophys. J. Int.,* **161**(2), 491–506.
Nakiboglu, S., 1982. Hydrostatic theory of the earth and its mechanical implications, *Phys. Earth planet. Inter.,* **28**(4), 302–311.
Parker, R.L., 1973. The rapid calculation of potential anomalies, *Geophys. J. Int.,* **31**(4), 447–455.
Parker, R.L. & Shure, L., 1985. Gravitational and magnetic fields of some simple solids of revolution, *Geophys. J. Int.,* **80**(3), 631–647.
Peltier, W.R., 1974. The impulse response of a maxwell earth, *Rev. Geophys.,* **12**(4), 649.
Phinney, R.A. & Burridge, R., 1973. Representation of the elastic—gravitational excitation of a spherical earth model by generalized spherical harmonics, *Geophys. J. Int.,* **34**(4), 451–487.
Saad, Y., 2003. *Iterative Methods for Sparse Linear Systems,* **Vol. 82,** SIAM.
Smith, M.L., 1977. Wobble and nutation of the earth, *Geophys. J. Int.,* **50**(1), 103–140.
Takeuchi, N., 2005. Finite boundary perturbation theory for the elastic equation of motion, *Geophys. J. Int.,* **160**(3), 1044–1058.
Van Loan, C.F. & Golub, G.H., 1983. *Matrix Computations,* Johns Hopkins University Press.
Wahr, J.M., 1981. Body tides on an elliptical, rotating, elastic and oceanless earth, *Geophys. J. R. astron. Soc.,* **64**(3), 677–703.
Waldvogel, J., 1979. The newtonian potential of homogeneous polyhedra, *Zeitschrift für angewandte Mathematik und Physik ZAMP,* **30**(2), 388–398.
Werner, R.A., 1994. The gravitational potential of a homogeneous polyhedron or don't cut corners, *Celest. Mech. Dyn. Astron.,* **59**(3), 253–278.
Woodhouse, J.H., 1976. On rayleigh's principle, *Geophys. J. Int.,* **46**(1), 11–22.
Woodhouse, J.H. & Dahlen, F.A., 1978. The effect of a general aspherical perturbation on the free oscillations of the Earth, *Geophys. J. Int.,* **53**(2), 335–354.

APPENDIX A: GENERALIZED SPHERICAL HARMONIC EXPANSIONS

Let (r, θ, φ) denote the usual spherical polar coordinates and $(\hat{\mathbf{r}}, \hat{\boldsymbol{\theta}}, \hat{\boldsymbol{\varphi}})$ the associated unit basis vectors. Following Phinney & Burridge (1973), we define the 'canonical basis vectors'

$$\hat{\mathbf{e}}_- = \frac{1}{\sqrt{2}}\left(\hat{\boldsymbol{\theta}} - i\hat{\boldsymbol{\varphi}}\right) \tag{A1}$$

$$\hat{\mathbf{e}}_0 = \hat{\mathbf{r}} \tag{A2}$$

$$\hat{\mathbf{e}}_+ = -\frac{1}{\sqrt{2}}\left(\hat{\boldsymbol{\theta}} + i\hat{\boldsymbol{\varphi}}\right), \tag{A3}$$

and write the contravariant components of a vector $\mathbf{u}$ with respect to this basis as u^-, u^0 and u^+. Each component can be expanded in the form

$$u^\alpha = \sum_{lm} u^\alpha_{lm} Y^\alpha_{lm}, \tag{A4}$$

where the Y^α_{lm} are the fully normalized generalized spherical harmonics defined in Appendix C of Dahlen & Tromp (1998) and summation is over integer values for $0 \le l \le \infty$ and $-l \le m \le l$.

A scalar field is expanded in terms of scalar spherical harmonics Y^0_{lm} in the usual fashion,

$$\phi = \sum_{lm} \phi_{lm} Y^0_{lm}, \tag{A5}$$

but we use generalized spherical harmonics to write the contravariant components of its gradient (a vector field) as

$$(\nabla\phi)^{\alpha} \equiv \sum_{lm} \phi_{lm}^{|\alpha} Y_{lm}^{\alpha}\,, \tag{A6}$$

where

$$\phi_{lm}^{|0} = \frac{d\phi_{lm}}{dr} \tag{A7}$$

and

$$\phi_{lm}^{|\pm} = \frac{k}{\sqrt{2}}\frac{\phi_{lm}}{r} \tag{A8}$$

with

$$k = \sqrt{l(l+1)}\,. \tag{A9}$$

The expansion of a second-rank tensor looks similar. By analogy, we define the contravariant components of $\mathbf{T}$ by

$$\mathbf{T} = \sum_{\alpha\beta} T^{\alpha\beta}\hat{\mathbf{e}}_{\alpha}\otimes\hat{\mathbf{e}}_{\beta} \tag{A10}$$

and expand each component as

$$T^{\alpha\beta} = \sum_{lm} T_{lm}^{\alpha\beta} Y_{lm}^{\alpha+\beta}\,. \tag{A11}$$

Thus T^{-+}, T^{+-} and T^{00} are all expanded in terms of the Y_{lm}^{0}, whilst, for example, T^{++} is expanded on Y_{lm}^{2}. We note in passing that the covariant components of the metric tensor are

$$g_{\alpha\beta} = \begin{pmatrix} 0 & 0 & -1 \\ 0 & 1 & 0 \\ -1 & 0 & 0 \end{pmatrix}. \tag{A12}$$

APPENDIX B: CALCULATION OF a FOR A RADIAL MAPPING

When the mapping $\boldsymbol{\xi}$ is radial, that is of the form

$$\boldsymbol{\xi}(\mathbf{x}) = \mathbf{x} + h(\mathbf{x})\hat{\mathbf{x}}\,, \tag{B1}$$

we can obtain a simple analytic expression for the components of $\mathbf{a}$ in terms of $(\nabla h)^{\alpha}$. The deformation gradient takes the form

$$\mathbf{F} = \left(1+\frac{h}{r}\right)\mathbf{1} + \mathbf{x}\otimes\left(\frac{1}{r}\nabla h - \frac{h}{r^2}\hat{\mathbf{x}}\right), \tag{B2}$$

whereupon we may use the Sherman–Morrison formula (e.g. Van Loan & Golub 1983) to write down an exact expression for the inverse:

$$\mathbf{F}^{-1} = \left(1+\frac{h}{r}\right)^{-1}\left(\mathbf{1} - \frac{\mathbf{x}\otimes\left(\frac{1}{r}\nabla h - \frac{h}{r^2}\hat{\mathbf{x}}\right)}{1+\partial_r h}\right). \tag{B3}$$

The matrix-determinant lemma (e.g. Van Loan & Golub 1983) yields the Jacobian,

$$J = \left(1+\frac{h}{r}\right)^{2}(1+\partial_r h)\,, \tag{B4}$$

and after a few more lines of algebra we find

$$\mathbf{a} = J\mathbf{C}^{-1} = (1+\partial_r h)\,\mathbf{1} + 2\frac{h}{r}\hat{\mathbf{r}}\otimes\hat{\mathbf{r}} - (\hat{\mathbf{r}}\otimes\nabla h + \nabla h\otimes\hat{\mathbf{r}}) + \frac{\|\nabla h - \frac{h}{r}\hat{\mathbf{r}}\|^2}{1+\partial_r h}\,\hat{\mathbf{r}}\otimes\hat{\mathbf{r}}\,. \tag{B5}$$

Expanding ∇h in the canonical basis and using the metric eq. (A12) to evaluate the norm, we arrive at

$$\left[a^{\alpha\beta}\right] = \begin{pmatrix} 0 & -(\nabla h)^{-} & -(1+\partial_r h) \\ -(\nabla h)^{-} & 1-\partial_r h + 2\dfrac{h}{r} + \dfrac{(\partial_r h - h/r)^2 - 2\,(\nabla h)^{-}\,(\nabla h)^{+}}{1+\partial_r h} & -(\nabla h)^{+} \\ -(1+\partial_r h) & -(\nabla h)^{+} & 0 \end{pmatrix}. \tag{B6}$$

Only if the mapping is radial can we use the Sherman–Morrison formula and matrix-determinant lemma. The reader may verify that the deformation gradient no longer takes the necessary form of 'identity plus tensor-product' when terms in $\hat{\boldsymbol{\theta}}$ and $\hat{\boldsymbol{\varphi}}$ are added to eq. (B1). It is of course possible to find an analytic expression for $a^{\alpha\beta}$ in more general cases; it is just not as elegant.